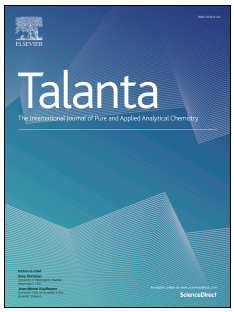

Electrostatic repulsion strategy for high-sensitive and selective determination of dopamine in the presence of uric acid and ascorbic acid

Ling Wang, Ran Yang, Lingbo Qu, Peter de B. Harrington

PII: S0039-9140(19)31259-7

DOI: https://doi.org/10.1016/j.talanta.2019.120626

Reference: TAL 120626

To appear in: *Talanta*

Received Date: 27 September 2019

Revised Date: 4 December 2019

Accepted Date: 7 December 2019

Please cite this article as: L. Wang, R. Yang, L. Qu, P.d.B. Harrington, Electrostatic repulsion strategy for high-sensitive and selective determination of dopamine in the presence of uric acid and ascorbic acid, *Talanta* (2020), doi: https://doi.org/10.1016/j.talanta.2019.120626.

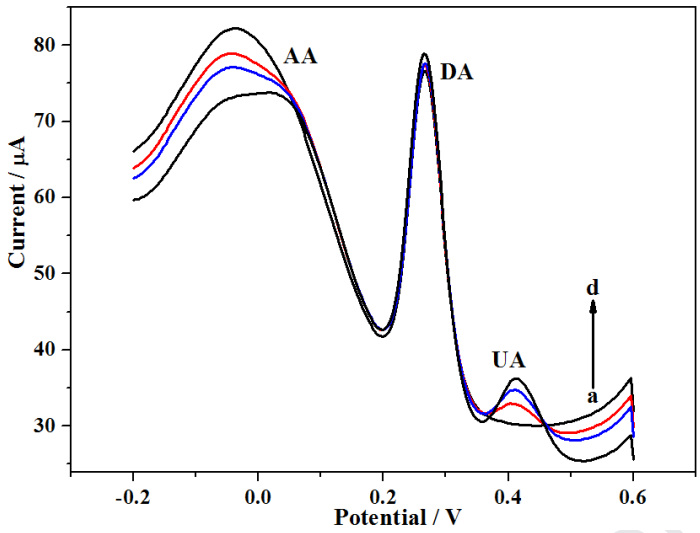

DPVs of 1.0 μmol L^{-1} DA in presence of different concentrations of AA and UA (a → d): 0, 20, 40, 120 μmol L^{-1}.

The poly(sodium 4-styrenesulfonate)-functionalized three-dimensional graphene (PFSG) composites were fabricated through a freeze-drying technique. The different electrical states between the modifier and the analyte were used to detect dopamine with high selectivity. The synergistic amplification of the enhanced electron transfer rate and the stronger surface attraction, the current signal of DA on PFSG/GCE was about 160 times enhanced compared with the bare electrode. Compared with previous electrochemical sensing, this method is more sensitive, selective, sensitive and simple.

Electrostatic repulsion strategy for high-sensitive and selective determination of dopamine in the presence of uric acid and ascorbic acid

Ling Wang [a,b], RanYang [b,*], Lingbo Qu [b], Peter de B. Harrington [c]

[a] *College of Chemistry and Chemical Engineering, Zhengzhou Normal University, Zhengzhou 450044, PR China*

[b] *College of Chemistry and Molecular Engineering, Zhengzhou University, Zhengzhou 450001, PR China*

[c] *Center for Intelligent Chemical Instrumentation, Department of Chemistry and Biochemistry, OHIO University, Athens, OH 45701-2979 USA*

*Corresponding Authors.
E-mail addresses: yangran@zzu.edu.cn (R. Yang).

Abstract:

In this work, poly(sodium 4-styrenesulfonate)-functionalized three-dimensional graphene (PFSG) composites were realized *via* a facile and green strategy. The nanocomposite was characterized by scanning electron microscopy, ultraviolet and visible spectroscopy, X-ray photoelectron spectroscopy, and electrochemical method. An electroanalytical sensor of dopamine (DA) with high sensitivity and selectivity was fabricated based on PFSG modified glassy carbon electrode (GCE). Under the optimum conditions, the negatively charged PFSG composites exhibit strong electrostatic attraction for DA and electrostatic repulsion to the negatively charged ascorbic acid (AA) and uric acid (UA) molecules. Such electrostatic interaction hindered the enrichment of AA and UA on the surface of PSFG/GCE, which make a higher selectivity for the DA even in the presence of 120-fold AA and UA. Owing to the enhanced electron transfer rate and the stronger surface attraction, the current signal of DA on PFSG/GCE was about 160 times enhanced compared with the bare electrode. There was a good linear relationship between the reduction peak current of DA and concentration across the range of 0.002 ~ 2.0 μmol L^{-1} and 2.0 ~ 10.0 μmol L^{-1} with the limit of 0.8 nmol·L^{-1}. Further, the PFSG/GCE was applied to the detection of DA in human serum samples. This biosensor is simple, sensitive, selective and highly stable, which provided a new design strategy and a valuable tool to detect DA in complex samples.

Keywords: Electrostatic repulsion strategy; Dopamine; Electrochemical sensor

1. Introduction

Dopamine (DA) is an important catecholamine neurotransmitter molecule that involved in the regulating of central nervous, hormone and cardiovascular system [1]. Normally, the concentrations of dopamine in brain fluids is in the range from 0.08 ~ 1.0 μmol L^{-1} [2]. Dysfunction of DA causes various diseases such as Parkinson's and Huntington's diseases [3]. Therefore, a sensitive and accurate quantification platform for DA levels in biological samples is of great urgent. Up to now, various analytical techniques including spectrofluorimetry [4], high-performance liquid chromatography [5], liquid chromatography-mass spectrometry[6] have been available for detection of DA. Compared to the above techniques, electro-analytical method is popular for its low cost, high sensitivity, and simplicity. However, uric acid (UA) and ascorbic acid (AA) often coexist with DA in the biological fluids and share similar oxidation potentials at bare electrode. On the other hand, for a healthy human being, the normal levels of DA, UA and AA in serum were 0.065 ~ 0.39 nmol L^{-1}, 0.24 ~ 0.52 mmol L^{-1} mmol L^{-1} and 0.03 ~ 36 mmol L^{-1}, respectively [7-9]. The concentrations of AA and UA are much higher than DA. The direct redox reactions of them are an irreversible process on bare electrodes, which inevitably foul the electrodes. As a result, poor selectivity and reproducibility are one of the urgent problems to be solved in the electrochemical detection of DA in the presence of such a high concentration of UA and AA. To overcome these obstacles, numerous nano-materials have been developed to construct modified electrode. From the comparison of the different modified electrodes for DA detection (Table 1) published in the last two years, it is found that the lower detection limits of DA were achieved at the Zn-NiAl LDH/rGO superlattice electrode. Nevertheless, the construction process of this sensor was tedious, which is not perfect enough in practice at present. Therefore, it is rurgent to establish a new

electrochemical sensing method for DA determination high sensitivity, selectivity and reproducibility.

Table 1

Three-dimensional (3D) graphene materials, which possess multilayer porous network structure, free-standing architecture with good mechanical strength as well as high electrical conductivity [25], have attracted considerable interest. As a promising materials for bio-sensing, Chen et al provided 3D graphene foam sensor for electrochemical sensing of DA with detection limit of 0.025 μmol L^{-1} [19]. However, most of the synthetic methods of three-dimensional graphene using chemical vapor deposition are complicated. A template-assisted self-assembly of GO following by chemical reduction was alternately an effective strategy to prepare three-dimensional graphene. Liu et al reported a 3D graphene modified GCE for DA determination with detection limit of 0.17 μmol L^{-1} [20]. There are two problems to be ameliorated in this work. One is chemical reduction process using hydrazine or dimethyl hydrazine that is a highly toxic and potentially explosive chemical. Another is the low detection sensitivity. A 3D arranged structure of graphene was obtained through freeze-drying a GO solution, in which adenosine was used as a functionalizing agent to inhibit the agglomeration of graphene sheets. Such a adenine-functionalized spongy graphene composite displayed highly sensitive and selective electrochemical responses to codeine phosphate [26] and the method is simple and environment-friendly. Poly(sodium 4-styrenesulfonate) (PSS) is an amphiphilic polymer. The π–π interaction between the graphene sheets and the aromatic rings of PSS, as well as the electrostatic repulsion between the negatively charged head groups of PSS, make the PSS functionalized graphene more stable and dispersive, which is beneficial to maintain the excellent performance of graphene. Here, the negatively charged

Poly(sodium 4-styrenesulfonate)-functionalized 3D graphene (PFSG) composites could attract the positively charged DA molecules (pK_a = 8.89) and repel the negatively charged AA (pK_a = 4.1) and UA (pK_a = 5.4) molecules [27]. Siriboon Mukdasai et al [28] has used similar principles to achieve the selective detection of tryptophan in the presence of AA and UA. Combined with the large surface area, fast electron transfer rate and the unique charge states of the spongy graphene, it is believed that PFSG has fascinating electrocatalytic potential for the DA.

According to the above design concept, in this work, negatively charged PSS functionalized spongy graphene (PFSG) was fabricated through a freeze-drying technique, in which PSS served as a stabilizer and ascorbic acid as a reducing agent. As expected, the resulting composite of PFSG exhibited amazing electro-catalytic activity and selectivity for redox of DA. In particular, compared with the sensing method reported, the reagent used is high environment-friendly and the construction process of this sensor is simple and easy to operate, which greatly improves the reproducibility and the possibility of practical application. The design concept of this sensor can provide a reference for the detection method for other analytical target molecules in complex biological samples.

2. Experimental

2.1. Reagents and apparatus

Graphite flake with the average diameter of 325 mesh was purchased from Alfa Aesar. PSS (MW = 70 000) and dopamine hydrochloride were obtained from Aladdin. Phosphate buffer solution (PBS) was prepared by mixing stock solutions of NaH_2PO_4, Na_2HPO_4 and KCl.

Cyclic voltammograms (CVs), differential pulse voltammograms (DPVs) and

electrochemical impedance spectroscopy (EIS) were obtained on an RST 5000 electrochemical workstation (Risetest, China) with three-electrode system. UV–vis spectra were collected on a T6 UV–Vis Spectrophotometers (Purkinje General, China). A sigma-500 field emission scanning electron microscope (Carl Zeiss, England) was used for imaging. X-ray photoelectron spectroscopy (XPS, Thermo Fisher Scientific ESCALAB 250Xi, USA) with an Al Ka X-ray source (1486.6 eV)

2.2. Synthesis of spongy graphene oxide (SGO)

The graphene oxide (GO) was prepared from natural graphite by a modified Hummers' method [29]. Generally, graphite (2.0 g) and H_2SO_4 (69 mL) were mixed under mechanical stirring for 30 min in an ice bath. $KMnO_4$ (8.0 g) was then added slowly and the mixture warmed to 35°C. After being sonicated vigorously for 12 h, 300 mL of water was added slowly, followed by the slow addition of 25 mL of 30% H_2O_2. The reaction mixture was filtered and washed with 5% HCl and water, respectively. To prepare spongy graphene oxide (SGO), the GO precipitate was dried with a freeze-dryer at a temperature of −53°C and a pressure of 10 Pa for three days [26, 30, 31].

2.3. Preparation of PSS functionalized spongy graphene (PFSG)

The PFSG was prepared by dispersing 50 mg SGO in water (20 mL). 500 mg PSS was added followed by stirring for more than 1 h. 200 mg of ascorbic acid was added and heated at 90°C for 3 h. Then, the mixture was centrifuged to remove excess PSS and reducing agents. The product was named as PFSG and was re-dispersed in distilled water for electrochemical experiment.

2.4. Preparation of real samples

Sample preparation was prepared with a slight modification according to the

literature [32]. Drug–free human blood was first centrifuged at 4000 rpm for 30 min. 1.6-mL aliquot of acetonitrile was added into a 0.5-mL aliquot of plasma sample and shaked for 1 min. The mixture was centrifuged at 10 000 rpm for 10 min to remove the protein. The supernatant was collected carefully and evaporated with nitrogen until dry. The residue was diluted in 5.0 mL of PBS and transferred into the electrolysis bath to be tested.

2.5. Fabrication of electrochemical sensor and electrochemical measurements

Prior to modification, the bare GCE was polished to a mirror-like with a 0.03 μm alumina slurry and washed cleanly. Then, 8-μL aliquot of 0.25 mg mL^{-1} PFSG dispersion was dropped onto the polished GCE surface and dried under an infrared lamp. For comparison, the SGO/GCE was prepared with the similar procedure.

In a typical process, the three-electrode system was immersed in PBS solution containing appropriate volume of DA or sample solution. The CVs or DPVs were recorded in the potential range from 0 V to 0.6 V with a scan rate of 0.10 V s^{-1} after accumulating for 240 s under stirring.

3. Results and discussion

3.1. Morphological and structural characterization of the PFSG

The morphology of the obtained nanocomposite was recorded by SEM. By comparing the SEM images of SGO (**Fig. 1A)** and PFSG (**Fig. 1B)**, it was found that no agglomeration of graphene was caused after reduction in the presence of PSS. **Fig. 1B** clearly displays the image of PFSG composite with interconnected, porous 3D framework of randomly oriented, wrinkled sheets. The 3D framework and crinkly sheets of PFSG can provide more active sites and increase specific surface area.

The UV-vis spectroscopy was used to confirm the obtained PFSG composite. As

can be seen in **Fig. 1B**, there is a strong absorption at 228 nm which referred to the $\pi-\pi^*$ transitions of C=C bonds and a shoulder peak at 300 nm which attributed to the $n-\pi^*$ transitions of C=O bonds [33, 34] for SGO. Under the same determination conditions, PSS has characteristic absorption at 226 nm and 262 nm [35]. In the case of PFSG, except for the characteristic absorption of PSS, the absorption peak at 228 nm is shifted to 269 nm. These data showed that the electronic conjugation within the graphene was restored upon the reduction by ascorbic acid and PSS successfully attached to the graphene surface.

Fig. 1.

In order to analyze the composition of PFSG composite, X-Ray photoelectron spectroscopy (XPS) was recorded. As shown in **Fig. 2A**, the XPS survey spectrum suggests that the PFSG nano-composite includes C, O, Na, and S elements. The characteristic peaks at ~167.4 eV (S 2p, corresponding to sulfonate) and ~1071.6 eV (Na 1s) were consistent with previous observations [35, 36], which clearly proved the the successful functionalization of the graphene sheets by PSS. In the high-resolution C 1s XPS spectrum (**Fig. 2B**), the deconvoluted four peaks at 284.6, 285.1, 286.7, and 289.4 eV, represent C–C, C–S, C=O, and C–C=O type bonds, respectively. Further, it can be seen obviously that the peak intensity of C=O and C–C=O is much lower than that of C–C, indicating that most of the oxygen-containing groups have been successfully removed after reduction interaction.

Fig. 2.

3.2. EIS studies

Electrochemical impedance spectroscopy (EIS) is widely used to study the interface characteristics of modified electrodes to further explore electron transfer

dynamics. The semicircle diameter of the Nyquist plots is equal to the electron-transfer resistance of the electrode surface [37]. **Fig. 3** showed the Nyquist plots of the bare GCE, SGO/GCE and PFSG/GCE electrodes recorded in 5.0 mmol L^{-1} $[Fe(CN)_6]^{3-/4-}$ solution containing 0.1 mol L^{-1} KCl. As can be seen, the semicircle diameter at SGO/GCE was much bigger than bare GCE due to the electrostatic repulsion between the oxygen-containing group in SGO film and $[Fe(CN)_6]^{3-/4-}$. However, the semicircle diameter at PFSG/GCE decreased obviously indicating that PFSG composite material greatly improved the electro-catalytic activity, which could be attributed to the extraordinary electron-transfer properties and the porous structure of PFSG that increased the specific surface area. The electrochemically effective electrode area of PFSG/GCE was calculated using chronocoulometry in a 1.0 mol L^{-1} of potassium ferrycianide solution. The effective area value of the PFSG/GCE was about 0.13 cm^2, which was significantly higher than that of the bare GCE (0.066 cm^2) and SGO/GCE (0.023 cm^2) under the same experimental conditions. These data proved that the introduction of PFSG nanocomposite played an important role in the increase of the electroactive surface area and providing the conducting bridges for the electron-transfer of $Fe(CN)_6^{3-/4-}$.

Fig. 3.

3.3. Cyclic voltammetric behavior of DA on the PFSG/GCE

Cyclic voltammetry was usually used to study the mechanism and performance of the electrochemical sensor. **Fig. 4** compares the CVs of different electrodes for DA. At the GCE, no obvious redox peaks for the DA were observed. When a layer of SGO was coated on the GCE surface, DA exhibits rather poor redox current peaks at E_{pa} = 0.3 V and E_{pc}= 0.18 V, which demonstrated the weaker adsorption and slower electrochemical reaction of DA on the SGO/GCE surface. However, in the case of

PFSG/GCE, a pair of well-defined and quasi-reversible redox peaks appeared at E_{pa} = 0.284 V and E_{pc}= 0.228 V under the same experimental condition, and the peak current increased obviously that are about 160 times higher than those at the bare GCE. No redox peaks were observed in the chosen potential domain for PFSG/GCE, which indicated that PFSG had no electro-activity. This superiority in analytical performance of the PFSG may be ascribed to the extraordinary electrontransfer properties as well as the structure of spongy graphene, which are favorable for DA adsorption and oxidation.

Fig. 4.

Fig. 5.

To prove the adsorption and enrichment of PFSG for DA, the reaction mechanism of the electrode reaction was first investigated by scanning the CV behaviors of DA at different scan rates (**Fig. 5**). As can be seen, both the oxidation (I_{pa}) and reduction (I_{pc}) peak current of DA linearly proportional to scan rates as well as their square root. The linear regression equations can be expressed as I_{pa} (μA) = 18.5 + 0.35 v (mV s^{-1}) (R^2 = 0.9802), I_{pc} (μA) = 9.9 + 0.42 v (mV s^{-1}) (R^2 = 0.9856), I_{pa} (μA) = −32.9 + 8.9 $v^{1/2}$ (mV s^{-1}) (R^2 = 0.9901), and I_{pc} (μA) = −52.2 + 10.8 $v^{1/2}$ (mV s^{-1}) (R^2 = 0.9826), respectively. However, the linearity were not very good, which suggest that the electrode reaction of DA might be controlled by both diffusion and adsorption [38]. For a diffusion and adsorption controlled electrode process, the saturating absorption capacity (Γ^*) of DA at electrode surface can be determined using chronocoulometry. The PFSG/GCE was immerged in a DA solution for 4 min and a step potential from 0.0 V to 0.6 V was applied. Then, the corresponding $Q-t$ curve was recorded. For contrast, $Q-t$ curve was also measured in blank PBS solution. **Fig. 5B** shows the $Q-t$ curves of the PFSG/GCE recorded in a blank and a DA

solution. The corresponding Q–$t^{1/2}$ plots were also performed and given in **Fig. 5C**. As can be seen in **Fig. 5C**, the intercepts and slopes were difference for blank and DA solution, further demonstrating that the electrode reaction process process of DA was controlled by both adsorption and diffusion [39]. The regression equations were given as: Q (10^{-4} C) = 7.18 $t^{1/2}$ + 5.19 (R^2 = 0.9968, curve b) and Q (10^{-4} C) = 2.89 $t^{1/2}$ + 1.67 (R^2 = 0.9959, curve a), respectively. According to the formula given by Anson [40] and the Laviron theory of $Q = nFA\Gamma^*$, the Γ^* value of 1.4×10^{-8} mol cm^{-2} was obtained. These data proved the enrichment of PFSG composite for DA.

3.4. Optimization of the experimental conditions

3.4.1. Effect of pH

The effect of pH values of the PBS solution in the range from 4.0 to 9.0 on the electrochemical responses of 3.0 μmol L^{-1} DA was investigated by cyclic voltammetry. In **Fig. 6**, the higher peak current of DA was obtained at a pH of 6.0. Therefore, PBS of pH 6.0 was chosen for further analytical measurements. As exhibited, the redox peak potentials shifted negatively by increasing of pH value, confirming that hydronium ions were directly participated in this electrode reaction process. The relation-ship between the redox peak potentials and pH can be expressed as: E_{pa} = − 0.0648 pH + 0.67 (R^2 = 0.9947) and E_{pc} = − 0.0589 pH + 0.59 (R^2 = 0.9994) (insert of Fig. 6). The slopes of the regression equations are close to the theory value of 0.059 V pH^{-1}, indicating that the same number of electrons and protons were involved in the electrochemical redox of DA on PFSG /GCE.

Fig. 6.

3.4.2. Effect of accumulation time

The influence of accumulation time was investigated in 3.0 μmol L^{-1} DA on PFSG/GCE. The results showed that the peak current of DA increased greatly with

with the accumulation time increase. When the accumulation time was longer than 240 s, the peak currents increased slowly. Considering the working efficiency and detection sensitivity, 240 s was chosen as the enrichment time.

3.5. Quantitative determination of DA based on differential pulse voltammetry

Under the optimal conditions, differential pulse voltammetry (DPV) was used for the determination of DA on the obtained electrochemical sensor. The differential pulse voltammograms (DPVs) of different concentrations of DA are shown in **Fig. 7A**. The inset of **Fig. 7A** is the corresponding calibration plot. The reduction peak current of DA is proportional to its concentration in the range from 0.002 to 2.0 μmol L^{-1} and 2.0 to 10.0 μmol L^{-1}. The corresponding linear regression equations were I_{pc} (μA) = 4.299 + 56.24 c (μmol L^{-1}) (R^2 = 0.9959) and I_{pc} (μA) = 93.9 + 15.25 c (μmol L^{-1}) (R^2 = 0.9757), respectively. Based on the signal-to-noise ratio of 3 (S/N), a detection limit of 0.8 nmol L^{-1} was be obtained. Compared with some modified electrode published in the last two years (Table 1), only Zn-NiAl LDH/graphene superlattice electrode [17] is as sensitive as this work reported. However, the synthesis of Zn-NiAl LDH/graphene superlattice nanohybride is very complicated. The fabrication process of this sensor proposed is simple and easy operation, which lays the foundation for reproducibility and stability, and also provides conditions for practical application. Therefore, the PFSG/GCE exhibited more excellent performance.

Fig. 7.

3.6. Stability, reproducibility and selectivity of the modified electrode

The stability and reproducibility of PFSG/GCE are examined using DPV. The fabrication reproducibility was evaluated by repeating the determination of a 10.0 μmol L^{-1} DA solution using six modified electrodes that were prepared independently under the same conditions, and the RSD was 4.5%. The long-term storage stability of

the PFSG/GCE was studied by monitoring its response to 3.0 μmol L^{-1} DA. A response of 90 % of the initial current was retained for the sensor after it was stored in dry environment for seven days. It indicated the good stability and reproducibility of the PFSG/GCE on DA.

To evaluate the practical application of the proposed method, the anti-interference performance of PFSG/GCE was further investigated. The tolerance limit was estimated to be less than 10% of the relative error for the current values at the peak potential of 1.0 μmol L^{-1} DA solution. The results demonstrated that 200-fold citric acid, 80-fold tryptophan and 40-fold phenylephrine hydrochloride concentrations did not interfere with the determination of DA. A number of inorganic ions, including Mg^{2+}, Ca^{2+}, Zn^{2+}, Mn^{2+}, SO_4^{2-} and NO_3^- had negligible effects on the determination.

Since UA and AA are usually oxidized at a nearly same potential with DA, the influence of AA and UA was evaluated using DPV technique. As exhibited in **Fig. 7B**, the cathodic peaks for AA, UA, and DA were clearly separated at PFSG/GCE. The peak currents of 1.0 μmol L^{-1} DA remained almost unchanged with adding UA and AA from 20 to 120 μmol L^{-1}. In pH 6.0, the PFSG composite repulsively interact with the negatively charged AA (pK_a = 4.1) and UA (pK_a = 5.4) and attractively interact with the positively charged DA (pK_a = 8.89). These studies suggest that controlling different electrical states between the modifier and the analytes is an effective strategy for selective detection of dopamine. Taken together, these results indicate that the sensor possesses excellent anti-interference ability and has good selectivity for DA detection.

3.7. Analytical application

The PFSG/GCE was finally applied to the analysis of DA by DPV to evaluate

practical utility of the proposed sensor. Since no electrochemical response of DA in human serum samples was observed, a standard addition method was used and each sample undergoes four parallel measurements. The results are summarized in **Table 2**. As a result, the obtained recoveries ranged between 86% and 88% and the RSD was less than 10%. These results indicated that the PFSG/GCE could be employed for trace analysis of DA in biological fluids.

Table 2

4. Conclusions

In summary, we have successfully synthesized the negatively charged PFSG composites and developed a highly selective and sensitive electrochemical sensor for detection of DA based on PFSG as a modifier. Relative to the reported methods, the sensor has lower detection limits and higher selectivity for AA, and is insensitive to AA and UA. These results prove that it is feasible to design a DA sensor with high sensitivity and selectivity by utilizing the charge state differences between the target molecule and the interferences. Therefore, it is anticipated that this sensor can be expanded easily as a simple and powerful tool for DA determination in complex samples.

Acknowledgement

This work was supported by National Natural Science Found of China (No. U1404214) and Henan Provincial Key Research Projects for Colleges and Universities (No. 20A150008).

References

[1] S. Yang, Y. Yin, L. Gang, Y. Ran, J. Li, L. Qu, Immobilization of gold nanoparticles on multi-wall carbon nanotubes as an enhanced material for selective voltammetric determination of dopamine, Sensors & Actuators B Chemical 178 (3) (2013) 217-221.

[2] R. Sivasubramanian, P. Biji, Preparation of copper (I) oxide nanohexagon decorated reduced

graphene oxide nanocomposite and its application in electrochemical sensing of dopamine, Materials Science & Engineering B 210 (2016) 10-18.

[3] C. Wang, R. Yuan, Y. Chai, Y. Zhang, F. Hu, M. Zhang, Au-nanoclusters incorporated 3-amino-5-mercapto-1,2,4-triazole film modified electrode for the simultaneous determination of ascorbic acid, dopamine, uric acid and nitrite, Biosensors & Bioelectronics 30 (1) (2011) 315-319.

[4] W. Hsin-Pin, C. Tian-Lu, T. Wei-Lung, Phosphate-modified TiO_2 nanoparticles for selective detection of dopamine, levodopa, adrenaline, and catechol based on fluorescence quenching, Langmuir the Acs Journal of Surfaces & Colloids 23 (14) (2007) 7880-7885.

[5] N. Ye, T. Gao, L. Jian, Hollow fiber-supported graphene oxide molecularly imprinted polymers for the determination of dopamine using HPLC-PDA, Analytical Methods 6 (18) (2014) 7518-7524.

[6] E.B. Aziza, K. Anders, A.R. Mohamed, Determination of dopamine and serotonin in human urine samples utilizing microextraction online with liquid chromatography/electrospray tandem mass spectrometry, Journal of Separation Science 30 (3) (2015) 421-424.

[7] J. Li, J. Yang, Z. Yang, Y. Li, S. Yu, Q. Xu, X. Hu, Graphene–Au nanoparticles nanocomposite film for selective electrochemical determination of dopamine, Analytical Methods 4 (6) (2012) 1725-1728.

[8] S.B. Khan, M.S. Ahmed, A.M. Asiri, Amperometric sensor for ascorbic acid using a gold electrode modified with ZnO@ SiO_2 nanospheres, New Journal of Chemistry 40 (10) (2016) 8438-8443.

[9] H. Devnani, N. Rashid, P.P. Ingole, Copper/Cuprous Oxide Nanoparticles Decorated Reduced Graphene Oxide Sheets Based Platform for Bio-Electrochemical Sensing of Dopamine, ChemistrySelect 4 (2) (2019) 633-643.

[10] Q. He, J. Liu, X. Liu, G. Li, D. Chen, P. Deng, J. Liang, A promising sensing platform toward dopamine using MnO_2 nanowires/electro-reduced graphene oxide composites, Electrochimica Acta 296 (2019) 683-692.

[11] A.A. Ganash, S.A. Alqarni, M.A. Hussein, Poly(aniline-co-o-anisidine)/graphene oxide Au nanocomposites for dopamine electrochemical sensing application, Journal of Applied Electrochemistry 49 (2) (2019) 179-194.

[12] S. Li, Y. Ma, Y. Liu, G. Xin, M. Wang, Z. Zhang, Z. Liu, Electrochemical sensor based on a three dimensional nanostructured MoS_2 nanosphere-PANI/reduced graphene oxide composite for simultaneous detection of ascorbic acid, dopamine, and uric acid, RSC Advances 9 (2019) 2997-3003.

[13] L. Jothi, S. Neogi, S. kumar Jaganathan, G. Nageswaran, Simultaneous determination of ascorbic acid, dopamine and uric acid by a novel electrochemical sensor based on N_2/Ar RF plasma assisted graphene nanosheets/graphene nanoribbons, Biosensors and Bioelectronics 105 (2018) 236-242.

[14] S. Ramki, K. Pandi, S.-M. Chen, Y.-T. Ye, T.-W. Chen, Q. Hao, Hydrothermal Synthesis of Manganese Sulfide Decorated Graphene Oxide for Effective Electrochemical Sensing of Dopamine, International Journal of Electrochemical Science, 14 (1) (2019) 1069-1081.

[15] S. Huang, S. Song, H. Yue, X. Gao, B. Wang, E. Guo, ZnO nanosheet balls anchored onto graphene foam for electrochemical determination of dopamine in the presence of uric acid, Sensors and Actuators B: Chemical 277 (2018) 381-387.

[16] P.V. Narayana, K. Rajshekhar, Enhanced electrochemical sensing of dopamine based on carboxylic acid functionalized multi-walled carbon nanotubes/poly(toluidine blue) composite, Synthetic Metals 245 (2018) 87-95.

[17] M. Asif, A. Aziz, H. Wang, Z. Wang, W. Wang, M. Ajmal, F. Xiao, X. Chen, H. Liu, Superlattice stacking by hybridizing layered double hydroxide nanosheets with layers of reduced graphene oxide for electrochemical simultaneous determination of dopamine, uric acid and ascorbic acid, Microchimica

Acta 186 (2) (2019) 61-71.

[18] Y. Zhao, J. Zhou, Z. Jia, D. Huo, Q. Liu, D. Zhong, Y. Hu, M. Yang, M. Bian, C. Hou, In-situ growth of gold nanoparticles on a 3D-network consisting of a MoS_2/rGO nanocomposite for simultaneous voltammetric determination of ascorbic acid, dopamine and uric acid, Microchimica Acta 186 (2019) 92-101.

[19] X. Dong, X. Wang, L. Wang, H. Song, H. Zhang, W. Huang, P. Chen, 3D graphene foam as a monolithic and macroporous carbon electrode for electrochemical sensing, ACS Appl Mater Interfaces 4 (6) (2012) 3129-3133.

[20] B. Yu, D. Kuang, S. Liu, C. Liu, T. Zhang, Template-assisted self-assembly method to prepare three-dimensional reduced graphene oxide for dopamine sensing, Sensors and Actuators B: Chemical 205 (2014) 120-126.

[21] T. Iranmanesh, M.M. Foroughi, S. Jahani, M.S. Zandi, H.H. Nadiki, Green and facile microwave solvent-free synthesis of CeO_2 nanoparticle-decorated CNTs as a quadruplet electrochemical platform for ultrasensitive and simultaneous detection of ascorbic acid, dopamine, uric acid and acetaminophen, Talanta 207 (2020) 120318-120334.

[22] S. Baluchová, A. Taylor, V. Mortet, S. Sedláková, L. Klimša, J. Kopeček, O. Hák, K. Schwarzová-Pecková, Porous boron doped diamond for dopamine sensing: Effect of boron doping level on morphology and electrochemical performance, Electrochimica Acta (2019) https://doi.org/10.1016/j.electacta.2019.135025.

[23] J. Shang, M. Zhao, H. Qu, H. Li, S. Chen, Fabrication of CQDs/MoS_2/Mo foil for the improved electrochemical detection, Analytica Chimica Acta 1079 (2019) 79-85.

[24] J. Gao, P. He, T. Yang, L. Zhou, X. Wang, S. Chen, H.Z. Hong Lei, Bin Jia, Jinfeng Liu, Electrodeposited NiO/graphene oxide nanocomposite: An enhanced voltammetric sensing platform for highly sensitive detection of uric acid, dopamine and ascorbic acid, Journal of Electroanalytical Chemistry (2019) https://doi.org/10.1016/j.jelechem.2019.113516.

[25] X.-B. Hu, Y.-L. Liu, W.-J. Wang, H.-W. Zhang, Y. Qin, S. Guo, X.-W. Zhang, L. Fu, W.-H. Huang, Biomimetic graphene-based 3D scaffold for long-term cell culture and real-time electrochemical monitoring, Analytical chemistry 90 (2) (2018) 1136-1141.

[26] M.A. Mohamed, D.M. El-Gendy, N. Ahmed, C.E. Banks, N.K. Allam, 3D Spongy Graphene-Modified Screen-Printed Sensors for the Voltammetric Determination of the Narcotic Drug Codeine, Biosensors & Bioelectronics 101 (2018) 90-95.

[27] A. Yang, Y. Xue, Y. Zhang, X. Zhang, H. Zhao, X. Li, Y. He, Z. Yuan, A simple one-pot synthesis of graphene nanosheet/SnO_2 nanoparticle hybrid nanocomposites and their application for selective and sensitive electrochemical detection of dopamine, Journal of Materials Chemistry B 1 (13) (2013) 1804-1811.

[28] S. Mukdasai, S. Poosittisak, W. Ngeontae, S. Srijaranai, A highly sensitive electrochemical determination of L-tryptophan in the presence of ascorbic acid and uric acid using in situ addition of tetrabutylammonium bromide on the ß-cyclodextrin incorporated multi-walled carbon nanotubes modified electrode, Sensors & Actuators B Chemical 272 (2018) 518-525.

[29] S. Bose, T. Kuila, M.E. Uddin, N.H. Kim, A.K.T. Lau, J.H. Lee, In-situ synthesis and characterization of electrically conductive polypyrrole/graphene nanocomposites, Polymer 51 (25) (2010) 5921-5928.

[30] D.M. El-Gendy, N.A.A. Ghany, E.E.F. El Sherbini, N.K. Allam, Adenine-functionalized Spongy Graphene for Green and High-Performance Supercapacitors, Scientific Reports 7 (2017) 43104-43113.

[31] X. Xu, L. Pan, Y. Liu, T. Lu, Z. Sun, D.H. Chua, Facile synthesis of novel graphene sponge for high performance capacitive deionization, Scientific reports 5 (2015) 8458-8466.

[32] C.X. Xu, K.J. Huang, Y. Fan, Z.W. Wu, J. Li, T. Can, Simultaneous electrochemical determination of dopamine and tryptophan using a TiO_2-graphene/poly(4-aminobenzenesulfonic acid) composite film based platform, Mat Sci Eng C-Mater 32 (4) (2012) 969-974.

[33] G. Yujing, G. Shaojun, R. Jiangtao, Z. Yueming, D. Shaojun, W. Erkang, Cyclodextrin functionalized graphene nanosheets with high supramolecular recognition capability: synthesis and host-guest inclusion for enhanced electrochemical performance, Acs Nano 4 (7) (2010) 4001-4010.

[34] C. Jin-Long, Y. Xiu-Ping, M. Kang, W. Shu-Feng, Graphene oxide based photoinduced charge transfer label-free near-infrared fluorescent biosensor for dopamine, Analytical Chemistry 83 (22) (2011) 8787-8793.

[35] S. Stankovich, R.D. Piner, X.Q. Chen, N.Q. Wu, S.T. Nguyen, R.S. Ruoff, Stable aqueous dispersions of graphitic nanoplatelets via the reduction of exfoliated graphite oxide in the presence of poly(sodium 4-styrenesulfonate), Journal of Materials Chemistry 16 (2) (2006) 155-158.

[36] A. Rani, K.A. Oh, H. Koo, H.J. Lee, P. Min, Multilayer films of cationic graphene-polyelectrolytes and anionic graphene-polyelectrolytes fabricated using layer-by-layer self-assembly, Applied Surface Science 257 (11) (2011) 4982-4989.

[37] G. Pelossof, R. Tel-Vered, S. Shimron, I. Willner, Controlling interfacial electron transfer and electrocatalysis by pH-or ion-switchable DNA monolayer-modified electrodes, Chemical Science 4 (3) (2013) 1137-1144.

[38] Y. Li, L. Zou, S. Ge, K. Li, B. Ye, Electrochemical behavior of sophoridine at a new amperometric sensor based on L-Theanine modified electrode and its sensitive determination, Journal of Electroanalytical Chemistry 709 (35) (2013) 1-9.

[39] W. Lu, Y. Li, G. Li, B. Ye, A new strategy for enhancing electrochemical sensing from MWCNTs modified electrode with Langmuir-Blodgett film and used in determination of methylparaben, Sensors & Actuators B Chemical 211 (2015) 332-338.

[40] F.C.Anson., Application of potentiostatic current integration to the study of the adsorption of cobalt(lll)-(ethylenedinitrilo)tetraacetate on mercury electrodes, Analytical Chemistry 36 (1964) 932-934.

Table 1 Comparison of the detection performance of PFSG/GCE with other sensors in the last two years.

Electrode	Linear range (μmol L^{-1})	Limit of detection (μmol L^{-1})	Ref.
MnO_2-graphene/GCE	0.01 ~ 0.10, 0.10 ~ 1.0, 1.0 ~ 80	0.001	[10]
AuNPs/PANI-co-PoAN/GO/Au electrode	5 ~ 100	0.0334	[11]
3D MoS_2-PANI/graphene/GCE	5 ~ 500	0.07	[12]
Cu/Cu_2O/graphene/GCE	0.25 ~ 17	0.0026	[9]
N2/Ar/graphene/GCE	0.01 ~ 400	0.0025	[13]
MnS/GO/GCE	0.04 ~ 138.07	0.007	[14]
ZnO/3D graphene foam electrode	1 ~ 80	0.01	[15]
MWCNTs-COOH/Poly(TB)/GCE	1 ~ 300	0.01	[16]
Zn-NiAl LDH/graphene superlattice/GCE	0.001 ~ 1	0.0001	[17]
3D-MoS_2/graphene/Au/GCE	0.3 ~ 198.3	0.11	[18]
3D graphene foam electrode	2.5 ~ 10.0	0.025	[19]
3D reduced graphene oxide/GCE	5 ~ 1000	0.17	[20]
CeO_2/CNT nano-composite/GCE	0.01 ~ 900	0.0031	[21]
Porous boron doped diamond	0.25 ~ 10.0	0.21	[22]
CQDs/MoS_2/Mo/GCE	0.1 ~ 100	0.05	[23]
NiO/GO/GCE	40 ~ 700	5.5	[24]

LDH: layered double hydroxide
TB: toluidine blue

Table 2 Determination of DA in human serum sample (n = 4).

Samples	Added (μmol L^{-1})	Found (μmol L^{-1})	RSD (%)	Recovery (%)
a	0	0	–	–
b	0.58	0.50±0.09	9.5	86
c	2.1	1.8±0.12	4.0	86
d	8.5	7.5±0.16	4.7	88

Figures and captions

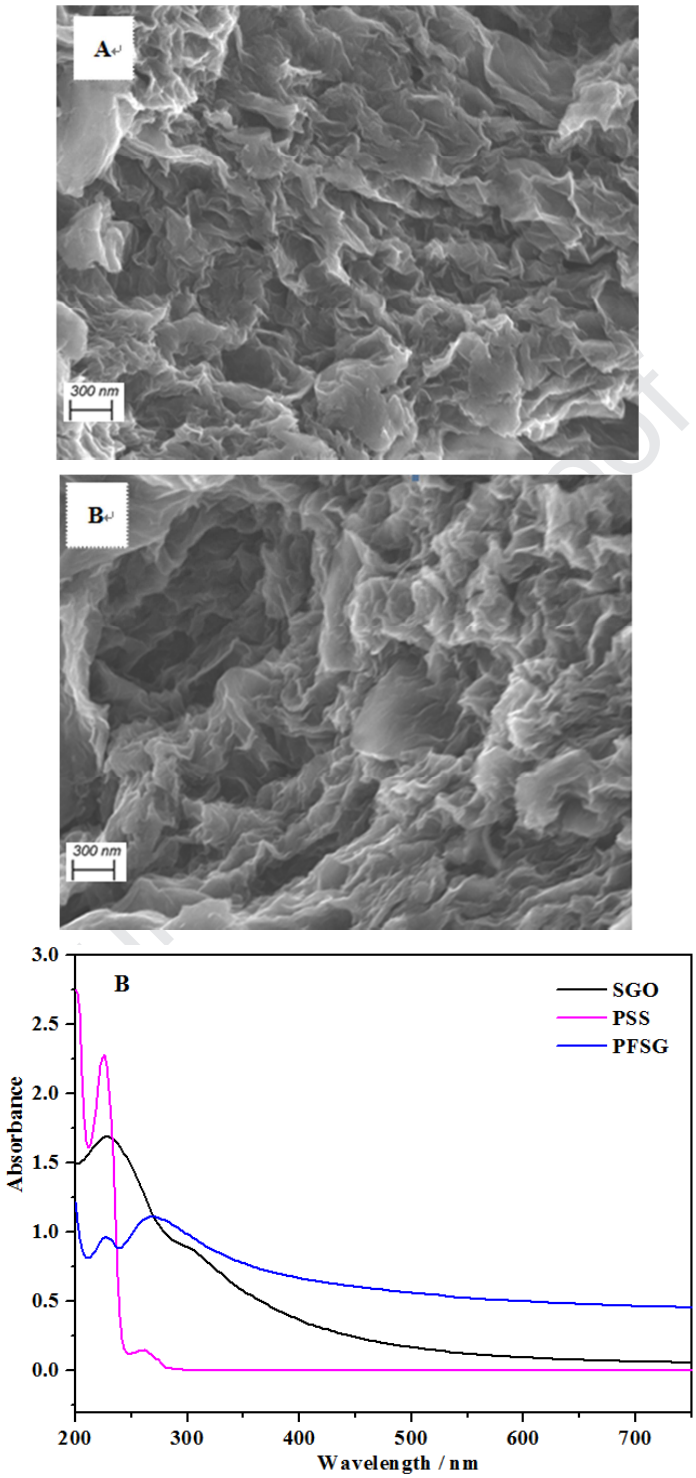

Fig. 1.

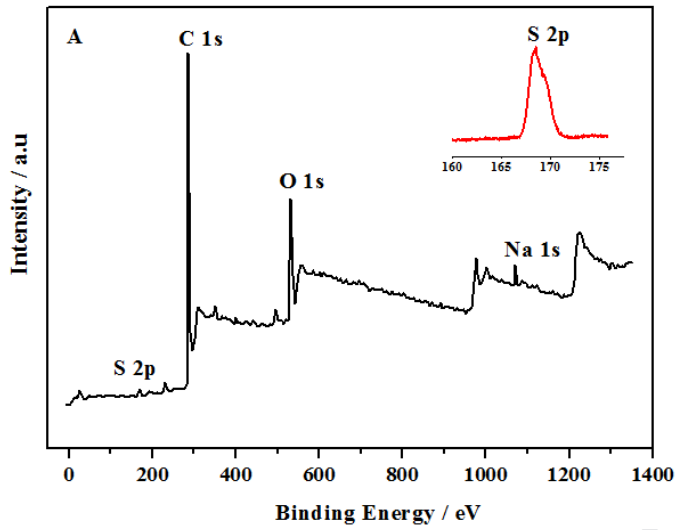
A
C 1s
S 2p
O 1s
Na 1s
S 2p
Intensity / a.u
0
200
400
600
800
1000
1200
1400
Binding Energy / eV
160
165
170
175

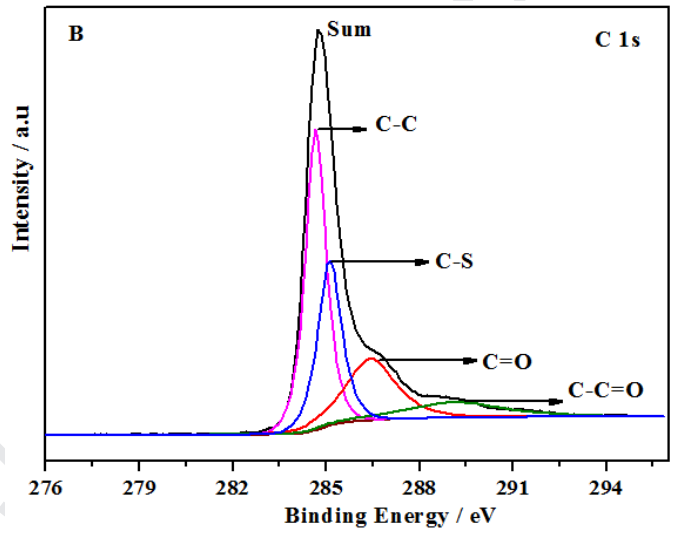
B
Sum
C 1s
C-C
C-S
C=O
C-C=O
Intensity / a.u
276
279
282
285
288
291
294
Binding Energy / eV

Fig. 2.

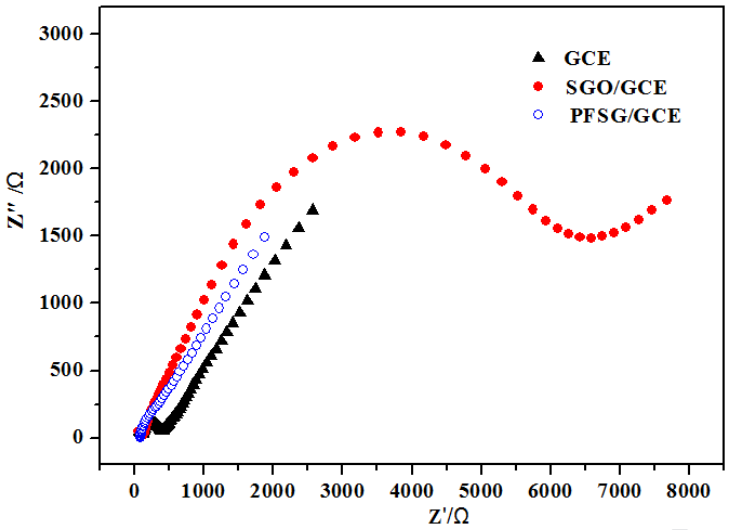
GCE
SGO/GCE
PFSG/GCE
Z'' /Ω
Z'/Ω
3000
2500
2000
1500
1000
500
0
0
1000
2000
3000
4000
5000
6000
7000
8000

Fig. 3.

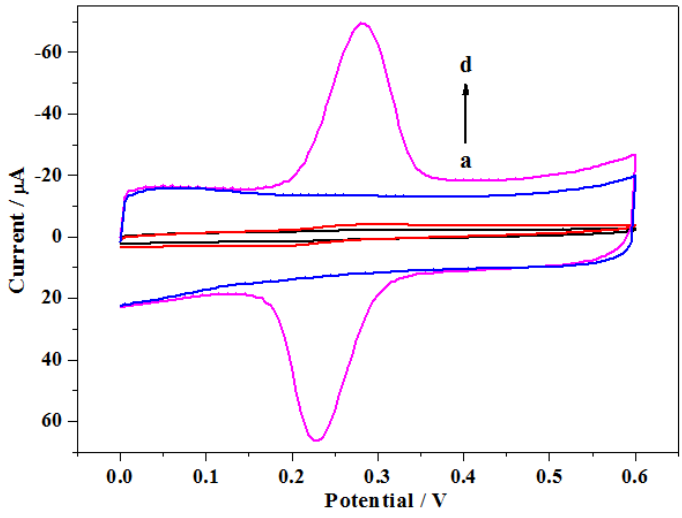
d
a
Current / μA
Potential / V
-60
-40
-20
0
20
40
60
0.0
0.1
0.2
0.3
0.4
0.5
0.6

Fig. 4.

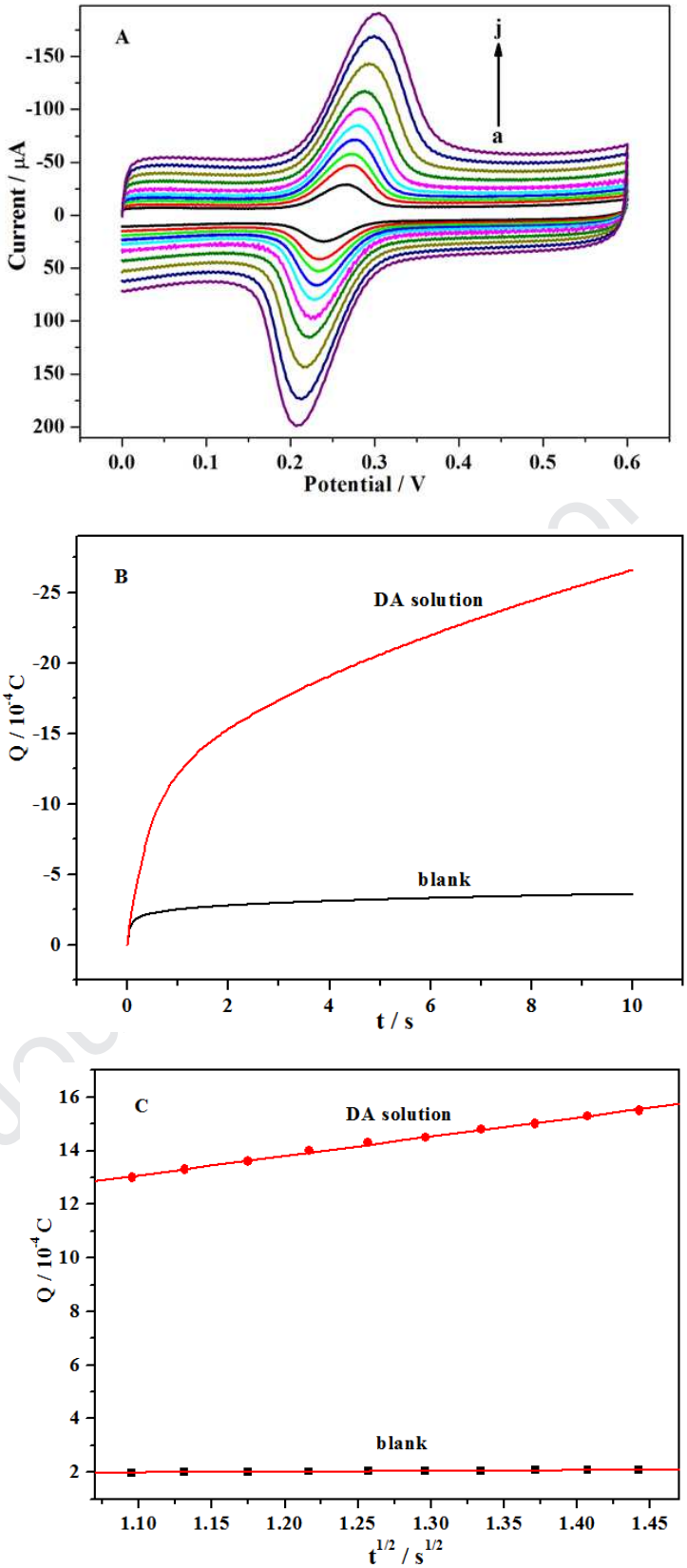
A
j
a
Current / μA
Potential / V
B
DA solution
blank
Q / 10^-4 C
t / s
C
DA solution
blank
Q / 10^-4 C
t^1/2 / s^1/2

Fig. 5.

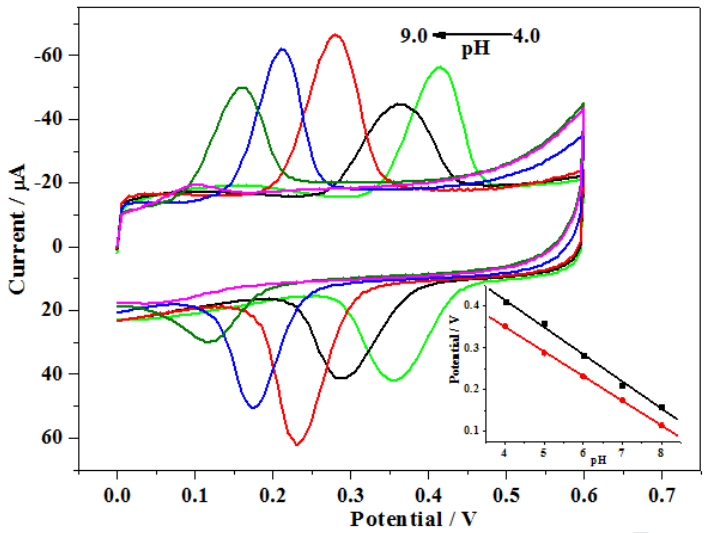

Fig. 6.

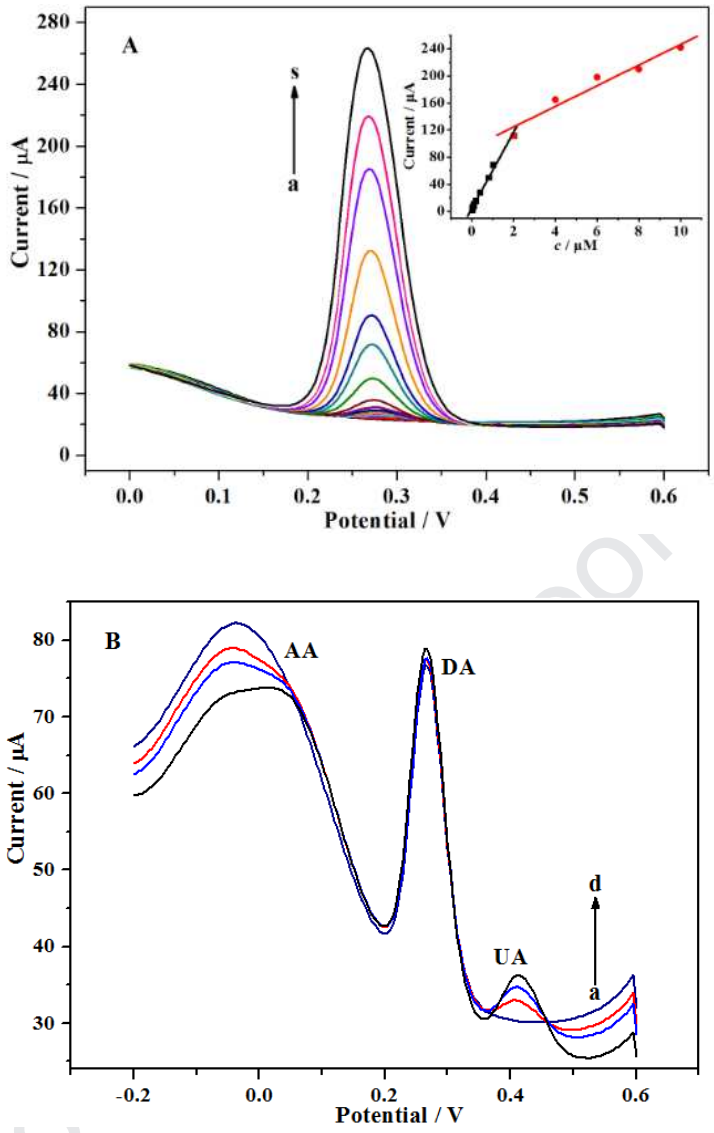
A
s
a
Current / μA
Potential / V
c / μM
B
AA
DA
UA
d
a
Current / μA
Potential / V

Fig.7.

Fig. 1. (A) SEM image of SGO composite. (B) SEM image of PFSG composite. (C) UV–Vis spectra of 0.1 mg mL^{-1} SGO, 0.12 mg mL^{-1} PSS and 0.025 mg mL^{-1} PFSG.

Fig. 2. XPS spetra of PFSF (a) and its C 1s (B) spectra. Inset is the higher resolution curve of S areas.

Fig. 3. Nyquist plots of EIS for bare GCE, SGO/GCE and PFSG/GCE.

Fig. 4. CVs of bare GCE (a), SGO/GCE (b), PFSG/GCE (d) in PBS with 3.0 μmol L^{-1} of DA and PFSG/GCE (c) in blank. Scan rate 0.10 V s^{-1}.

Fig. 5. (A) CVs of 3.0 μmol L^{-1} DA at the PFSG/GCE with different scan rates (a → i): 40, 60, 80, 100, 120, 150, 200, 250, 300, 350 mV s^{-1}. (B) Chronocoulometric response curves abtained at the PFSG/GCE in blank and DA solution. (C) The relationship of charge Q vs. $t^{1/2}$.

Fig. 6. Cyclic voltammograms of the PFSG/GCE in the presence of 3.0 μmol L^{-1} DA at different pH of PBS. Inset the redox peak potential with respect to pH. Scan rate 100 mV s^{-1}.

Fig. 7. (A) DPVs of DA at PFSG/GCE with different concentrations (a→s): 0.0, 0.002, 0.004, 0.006, 0.01, 0.02, 0.04, 0.06, 0.08, 0.1, 0.2, 0.4, 0.8, 1.0, 2.0, 4.0, 6.0, 8.0, 10.0 μmol L^{-1}. Inset is the calibration curve. (B) DPVs of 1.0 μmol L^{-1} DA in presence of different concentrations of AA and UA (a → d): 0, 20, 40, 120 μmol L^{-1}.

Highlights

1. Using different electrical states between the modifier and the analyte, the highly selective detection of dopamine was realized.

2. The current signal of DA on PFSG/GCE was about 160 times enhanced compared with the bare GCE.

3. This established method is selective, sensitive and simple.

Declaration of interests

☑The authors declare that they have no known competing financial interests or personal relationships that could have appeared to influence the work reported in this paper.

☐The authors declare the following financial interests/personal relationships which may be considered as potential competing interests: